Non-Invasive Ultrasonic Tomography: Liquid/Gas Flow Visualization

[1]R. Abdul Rahim, [2]M.H. Fazalul Rahiman, and [2]M.N. Mohd Taib

[1]Control and Instrumentation Engineering Department,
Faculty of Electrical Engineering, Universiti Teknologi Malaysia,
81300 Skudai, Johor, Malaysia.
ruzairi@fke.utm.my

[2]Mechatronic Engineering Department,
Faculty of Engineering Industry, Universiti Industri Selangor (UNISEL),
40000 Shah Alam, Selangor, Malaysia.
hafizfr@yahoo.com

***Abstract*—This paper presents the non-invasive ultrasonic tomography system for imaging liquid and gas flow. Transmission-mode approach has been used for sensing the liquid/gas two-phase flow, which is a kind of strongly inhomogeneous medium. The algorithms used to reconstruct the concentration profile for two-phase flow using fan-shaped beam scanning geometry were presented. Experiments showed that the performance of the system is acceptable. Results of the experiments using LBPA, HRA and HBRA were discussed.**

Keywords—Flow Imaging, Image Reconstruction, Non-invasive, Ultrasonic

I. INTRODUCTION

Real-time process monitoring plays a dominant role in many areas of industry and scientific research concerning liquid/gas two-phase flow. It is proved that the operation efficiency of such process is closely related to accurate measurement and control of hydrodynamic parameters such as flow regime and flow rate [1]. Besides, monitoring in the process industry has been limited to either visual inspection or single point product sampling where product uniformity is assumed.

Ultrasonic Tomography has the advantage of imaging two-component flows where the major potential benefits are, it is possible to gain an insight into the actual process. Besides, since Ultrasonic Tomography is capable of on-line monitoring, it is the opportunity to develop closed loop control systems and finally, it can be non-invasive and possibly non-intrusive system [3], [8].

Manuscript received June 9, 2005. This work was supported in part by the Malaysian Government under IRPA Grant Vot. 74188. The authors are grateful to Malaysian Government for providing research grant under IRPA Vot. 74188. M.H. Fazalul Rahiman and M.N. Mohd Taib would like to thanks Universiti Industri Selangor (UNISEL), Malaysia for the contribution to publish this paper.

The work reported in this paper demonstrates image reconstruction techniques applied to an experimental vessel of liquid/gas flow using non-invasive Ultrasonic Tomography technique. The introduction is firstly described. Second, the Ultrasonic Tomography modelling is explained. Third, the measurement system is put forward. Fourth, the image reconstruction algorithms are briefly discussed and the results obtained are presented. Finally the discussions for the results are presented.

II. ULTRASONIC TOMOGRAPHY MODELLING

Process tomography can be used to obtain both qualitative and quantitative data needed in modelling a multi-fluid flow system. The modelling is carried out to predict the spatial and temporal behaviour of a process and it becomes more significant as the inherent complexity of a process increases [9]. A useful descriptor of the interaction of ultrasound with a material is its acoustic impedance (the complex ratio of sound pressure to particle velocity), which is analogous to electrical impedance [2]. The acoustic impedance (Z) is described as:

$$Z = \rho c \tag{1}$$

where Z = the acoustic impedance (kg/m^{2}s), ρ = the density of the medium (kg/m^3) and c = the sound velocity in the medium (m/s). The greater the difference in acoustic impedance at interface, the greater will be the amount of energy reflected. Conversely, if the impedances are similar, most of the energy is transmitted. The system presented here utilized transmission-mode measurement of transmitted signal amplitude with fan-shaped beam profiles on the assumption that the ultrasonic wave propagates in a straight line. The fan-shaped beam profiles of the system are shown in figure 1. Due

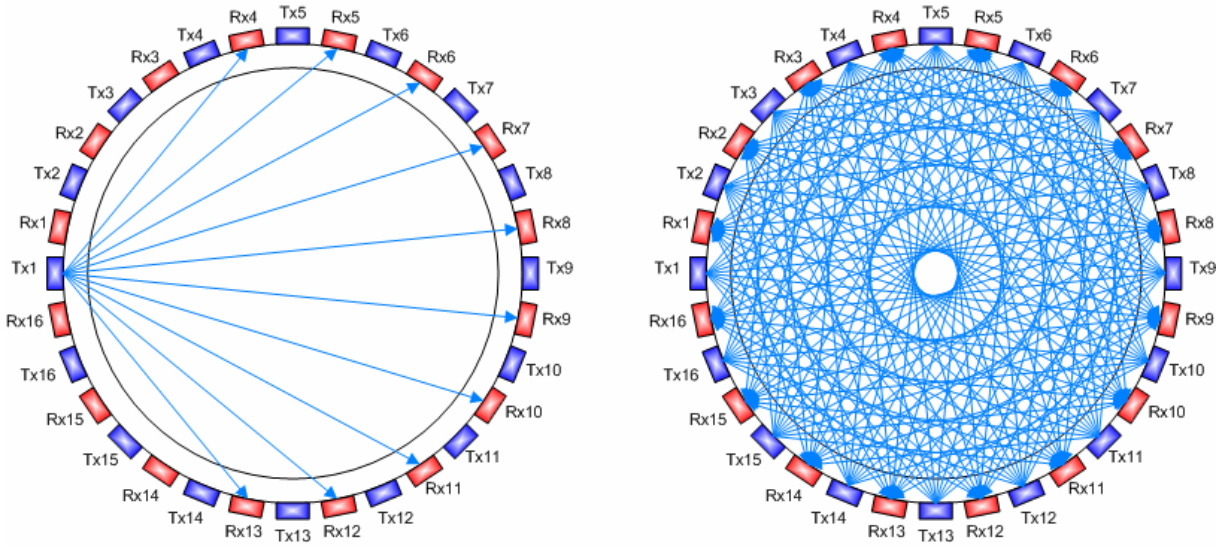

Fig. 1. Single projection view (left) and 16 projections view (right)

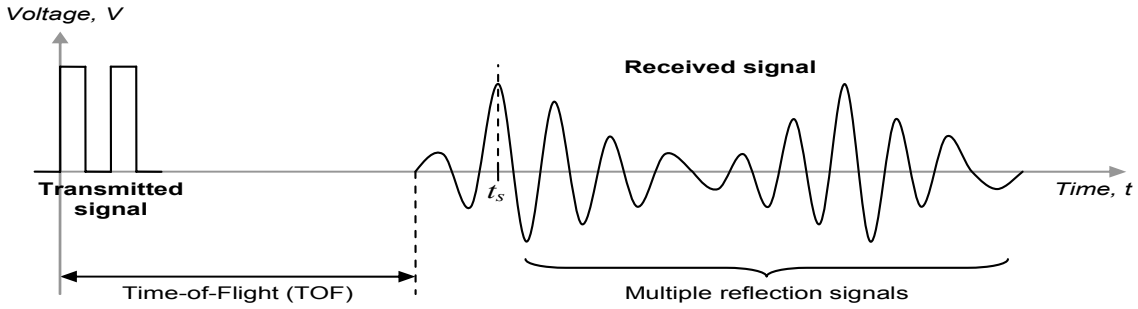

Fig. 2. Example of a transmitter and a receiver signal

to significant of acoustic impedance mismatch between two components of liquid and gas flow, ultrasound incident wave on a water and gas boundary for example is over 99.97% reflected [6].

The gas hold-ups in the measurement section should be greater than at least half of the ultrasonic wavelength to block the ultrasonic energy from reaches the receiver during the measurement period [11]. The significant relationship for the ultrasonic wavelength is shown as below:

$$v = f\lambda \tag{2}$$

where v = speed of sound (m/s), f = ultrasonic frequency (Hz) and λ = the wavelength (m). In this system, a 40kHz transducer frequency, (f) is chosen and it is known that the speed of sound, (v) in water at 25^{o}C is 1500m/s. Thus, the ultrasonic wavelength obtained which is shown by (2) is approximately 38mm. From the previous quotation, the resolution for the transducer was set to half-wavelength resulting transducer resolution of 19mm. Therefore, the gas hold-up size or the gas bubbles should be at least 19mm in average or it could not sensed by the ultrasonic sensing array. On the other hand, the sensor loss voltage (attenuation) increases proportionally to the size of gas cavity whereby the gas cavity blocks the ultrasound energy transmitted to the receiver. Therefore the receiver voltage (sensor value) is decreased as the sensor loss voltage increased.

The arrival time method has been used. Arrival time analysis is based on the simple fact that it takes some finite time for an ultrasonic disturbance to move from one position to another inside the experimental pipe. In figure 2, the *observation time* denoted by t_s is the first peak after the time-of-flight corresponding to a straight path. When a pulse is transmitted, for each receiver there is a specific observation time at which the transmitted pulse should arrive. By sampling the amplitude of this observation time for every receiving sensor, the information via transmission-mode method can be obtained [4].

III. THE MEASUREMENT SYSTEM

The most common elements used in tomography field are the PZT-5A piezoelectric material with 2MHz resonance frequency [4], [6]. This type of element usually excited at 200V by using a triode avalanche-based switch circuit [6]. For this system, the active element for the transducers is the

ceramic piezoelectric with resonance frequency of 40 kHz. The success of all acoustic imaging systems lies in matching the properties of the imaged objects with the related characteristics of ultrasound. In practice, if an ultrasonic transducer is placed against the surface of a material, very little ultrasonic energy will actually enter the material [7]. This is because a very thin air layer will usually exist between the face of the transducer and the surface of the material. Air, being a very poor conductor of sound energy, will prevent effective coupling of the transducer to the material. For this reason, some sort of coupling material is normally used. Normally a liquid (wet coupling) is used to allow easy application and conformity to the void between the transducer and the surface. It also should be a very good conductor of sound energy to allow maximum transfer to the structure [8].

The sensing area has been developed by using 16-pairs of ultrasonic transducers and the designation is shown in figure1. The Tx1, Tx2, Tx3 and etc. represents the transmitters whereas the Rx1, Rx2, Rx3 and etc. represents the receivers. The transducers are mounted on an acrylic pipe and the silicon grease has been used as the couplant. The ultrasonic transmitters will transmit pulses at 40 kHz through the process vessel to the point of interest. Each transmitter excited will emit two cycles of tone burst of 40 kHz at 20Vp-p. These transducers having divergence angle of 125^{o} resulting each projection from the transmitting transducers cover up to 10-channels of the receiving transducers. A total of 16 observations are made in one scan, hence 160 independent measurements were obtained for one full scan.

IV. IMAGE RECONSTRUCTION

In order to reconstruct the cross section images plane from the projection data, back projection algorithm has been employed. Basically, the measurements obtained at each projected data are the attenuated sensor values due to object space in the image plane. These sensor values are then back projected by multiply with the corresponding normalized sensitivity maps. The back projected data values are smeared back across the unknown density function (image) and overlapped to each other to increase the projection data density.

A. Linear Back Projection Algorithm

In Linear Back Projection Algorithm (LBPA), the concentration profile is generated by combining the projection data from each sensor with its computed sensitivity maps. The modelled sensitivity matrices are used to represent the image plane for each view. To reconstruct the image, each sensitivity matrix is multiplied by its corresponding sensor loss value; this is same as back project each sensor loss value to the image plane individually [5]. Then, the same elements in these matrices are summed to provide the back projected voltage distributions (concentration profile) and finally these voltage distributions will be represented by the colour level (coloured pixels). This process can be expressed mathematically as below:

$$V_{LBP}(x,y) = \sum_{Tx=1}^{16}\sum_{Rx=1}^{16} S_{Tx,\,Rx} \times \overline{M}_{Tx,\,Rx}(x,y) \tag{3}$$

where $V_{LBP}(x, y)$ = voltage distribution obtained using LBP algorithm in the concentration profile matrix, $S_{Tx,Rx}$ = sensor loss voltage for the corresponding transmission (Tx) and reception (Rx) and $\overline{M}_{Tx,\,Rx}(x,y)$ is the normalized sensitivity map for the view of Tx to Rx.

B. Hybrid Reconstruction Algorithm

The Hybrid Reconstruction Algorithm (HRA) is based on the previous development by Ibrahim [10]. This algorithm determines the condition of projection data and improves the reconstruction by marking the empty area during image reconstruction.

As a result, the smearing effect caused by the back projection technique is reduced. The HRA is obtained by multiplying the concentration profile obtained using the LBPA with the HRA masking matrix. The HRA masking matrix was obtained by filtering each of the concentration profile element. If the concentration profile element is larger or equal to ¾ of the maximum pixel value, then the masking matrix element for the corresponding concentration profile element is set to one otherwise it is set to zero. The mathematical model for HRA is shown by (4) and (5).

$$V_{HRA}(x,y) = B_{HRA}(x,y) \times V_{LBP}(x,y) \tag{4}$$

In which:

$$\begin{aligned} B_{HRA}(x,y) = 0 &\Rightarrow V_{LBP}(x,y) < P_{Th} \\ B_{HRA}(x,y) = 1 &\Rightarrow V_{LBP}(x,y) \geq P_{Th} \end{aligned} \tag{5}$$

where $B_{HRA}(x, y)$ = HRA masking matrix, P_{Th} = pixel threshold value (¾ of the maximum value), $V_{LBP}(x, y)$ = reconstructed concentration profile using LBPA and $V_{HRA}(x, y)$ = improved concentration profile using HRA.

C. Hybrid-Binary Reconstruction Algorithm

For comparison with the LBPA and HRA method, another image reconstruction technique has been employed namely the Hybrid-Binary Reconstruction Algorithm (HBRA). This algorithm has the advantage of improving the stability and repeatability of the reconstructed image. The HBRA is obtained by multiplying each sensor value to its corresponding sensitivity map. If the sensor value is higher or equal to the threshold voltage, (V_{Th}) then its projection path which is represented by the sensitivity map is set to a maximum pixel value (511), otherwise it is set to a minimum pixel value (0). This threshold voltage is needed for the purpose of separating the object from the background, thus creating a binary picture from a picture data (tomogram). This procedure is only

appropriate for two-phase flow imaging in cases where the phases are well separated such as liquid-gas flow [1]. The mathematical model for HBRA is shown as follows:

$$V_{HBR}(x,y) = \sum_{Tx=1}^{16}\sum_{Rx=1}^{16} V_{Tx,\,Rx} \times \overline{M}_{Tx,\,Rx}(x,y) \tag{6}$$

In which:

$$\begin{aligned} V_{HBR}(x,y) &= 0 \quad \Rightarrow V_{Tx,\,Rx} < V_{Th} \\ V_{HBR}(x,y) &= 511 \quad \Rightarrow V_{Tx,\,Rx} \geq V_{Th} \end{aligned} \tag{7}$$

where $V_{Tx,Rx}$ = the sensor value and $V_{HBR}(x, y)$ = concentration profile obtained using HBRA.

The dynamic characteristics of liquid-gas flow are most probably uncertain and it is quite hard to predict the behaviour of such flow. For industrial flows, the sudden changes in terms of pressure lead to wavy flow. This may result the sensor value to fluctuate randomly and causes to the unknown image reconstructed as well as increases the measurement error. By thresholding the sensor value, it limits the sensor value fluctuation and therefore minimizes the measurement error.

D. Experiments

The LBPA, HRA and HBRA have been tested with a number of static test profiles. The reconstruction results for two gas hold-ups is shown in figure 3, bubbly flow in figure 4, half liquid flow in figure 5, annular flow in figure 6 and slug flow in figure 7.

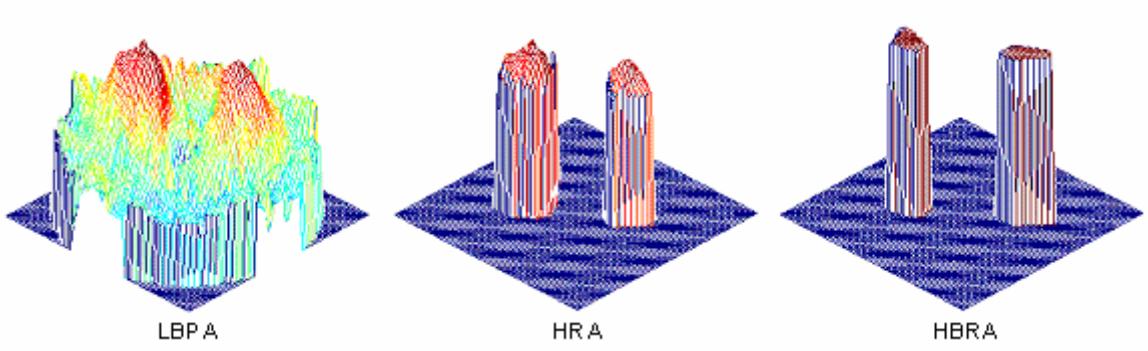

Fig. 3. Image reconstructed for two gas hold-ups

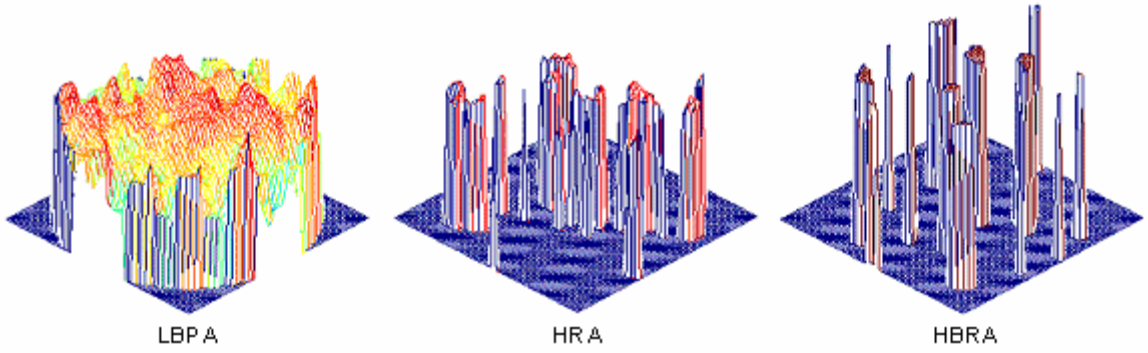

Fig. 4. Image reconstructed for bubbly flow

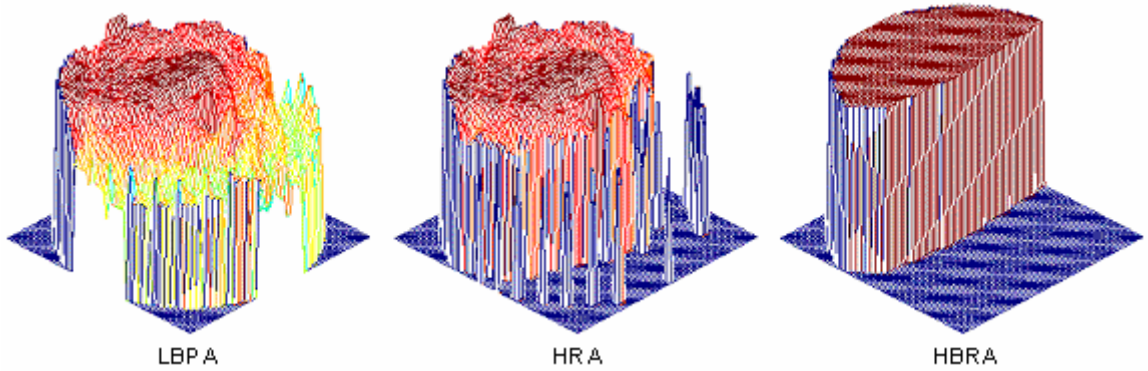

Fig. 5. Image reconstructed for half liquid flow

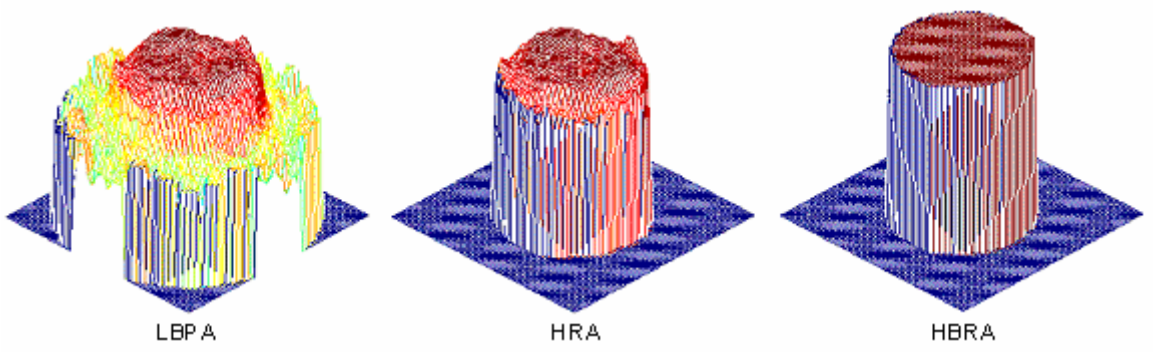

Fig. 6. Image reconstructed for annular flow

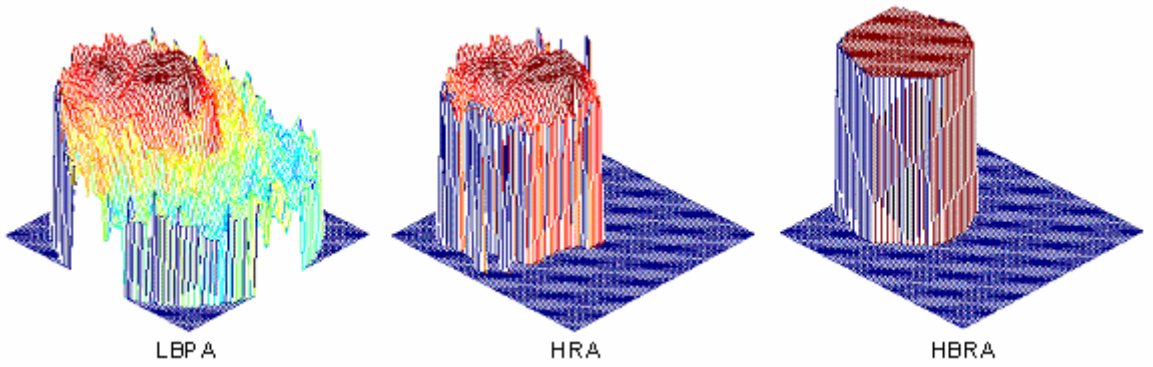

Fig. 7. Image reconstructed for slug flow

V. Discussions

As seen in the results presented, LBPA smears out elsewhere and resulting blurry image. Hence, it is very hard to obtain quantitative information from this image. This major drawback of LBPA however has been improved by using HRA technique. From the reconstructed images, it shown that blurry image by the smearing effects has been cut down. Though, the blurry image still exists among high pixel value. Basically, HRA and LBPA sharing the same concentration profile matrix, except that the HRA has an integrated threshold filter. This threshold filter will cut off pixel value lower than 383 pixel values resulting less blurry image. For higher pixel value blurring, the HRA will fail. The developed HBRA however tends to eliminate all the smearing effects and it is proven in the previous experiments. From the overall reconstructed images, HBRA was found excellent in reconstructing liquid and gas two-phase flow.

References

[1] A. Plaskowski, M.S. Beck, R. Thron, and T. Dyakowski, "Imaging Industrial Flows: Applications of Electrical Process Tomography," U.K.: IOP Publishing Ltd., 1995.

[2] B.S. Hoyle, "Process Tomography Using Ultrasonic Sensors," *Journal Measurement Science Technology*, vol. 7, pp. 272-280, 1996.

[3] B.S. Hoyle, and L.A, Xu, "Ultrasonic Sensors," in R.A. Williams and M.S. Beck, *Process Tomography: Principles, Techniques and Applications*, Oxford: Butterworth-Heinemann, pp. 119-149, 1995.

[4] H. Gai, Y.C. Li, A. Plaskowski, and M.S. Beck, "Ultrasonic Flow Imaging Using Time-Resolved Transmission-Mode Tomography," *Proc. IEE 3rd International Conference on Image Processing and Its Applications*, Warwick: Warwick University Press, pp. 237-241, 1989.

[5] K.S. Chan, "Real-Time Image Reconstruction for Fan Beam Optical Tomography System," M.Eng. Thesis, Universiti Teknologi Malaysia, 2002.

[6] L. Xu, Y. Han, L.A. Xu, and J. Yang, "Application of Ultrasonic Tomography to Monitoring Gas/Liquid Flow," *Journal Chemical Engineering Science*, vol. 52, pp. 2171-2183, 1997.

[7] M.L. Sanderson, and H. Yeung, "Guidelines for the Use of Ultrasonic Non-Invasive Metering Technique," *Journal Flow Measurement and Instrumentation*, vol. 13, pp. 125-142, 2002.

[8] R. Abdul Rahim, M.H. Fazalul Rahiman, and K.S. Chan, "Monitoring Liquid/Gas Flow Using Ultrasonic Tomography," *Proc. 3rd International Symposium on Process Tomography in Poland*, Lodz, Poland, pp.130-133, 2004.

[9] R.M. West, S. Meng, R.G. Aykroyd, and R.A. Williams, "Spatial-Temporal Modelling for Electrical Impedance Imaging of a Mixing Process," *Proc. 3rd World Congress on Industrial Process Tomography*, Banff, Canada, pp. 226-232, 2003.

[10] S. Ibrahim, "Measurement of Gas Bubbles in a Vertical Water Column Using Optical Tomography," Ph.D Thesis, Sheffield Hallam University, 2000.

[11] W. Warsito, M. Ohkawa, N. Kawata, and S. Uchida, "Cross-Sectional Distributions of Gas and Solid Holdups in Slurry Bubble Column Investigated by Ultrasonic Computed Tomography," *Journal Chemical Engineering Science*, vol. 54, pp. 4711-4728, 1999.